PERGAMON

Available online at www.sciencedirect.com

SCIENCE DIRECT®

Polyhedron 22 (2003) 35–44

POLYHEDRON

www.elsevier.com/locate/poly

# Titania and tungsten doped titania thin films on glass; active photocatalysts

Ashti Rampaul [a], Ivan P. Parkin [a,*], Shane A. O'Neill [a], Juilio DeSouza [a], Andrew Mills [b], Nickolas Elliott [b]

[a] *Christopher Ingold Laboratory, Department of Chemistry, University College London, 20 Gordon Street, London WC1H OAJ, UK*
[b] *Department of Chemistry, University of Strathclyde, Thomas Graham Building, 295 Cathedral Street, Glasgow G1 1XL, UK*

Received 20 June 2002; accepted 21 October 2002

**Abstract**

Acidification of an isopropanol solution containing mixtures of $[Ti(OPr^i)_4]$ and $[W(OEt)_5]$ produced solutions from which various $TiO_2$, $WO_3$ and $TiO_2/WO_3$ thin films could be obtained by dip coating and annealing. The films were analysed by X-ray diffraction, SEM/EDAX, Raman, electronic spectra, contact angle and photoactivity with respect to destruction of an over layer of stearic acid. The $TiO_2/WO_3$ films were shown to be mixtures of two phases $TiO_2$ and $WO_3$ rather than a solid solution $Ti_xW_yO_2$. The 2% tungsten oxide doped titania films were shown to be the most effective photocatalysts. All of the $TiO_2$ and $TiO_2/WO_3$ films showed light induced superhydrophillicity.
© 2002 Elsevier Science Ltd. All rights reserved.

*Keywords:* Titania; Photocatalyst; Electronic spectra; Stearic acid

## 1. Introduction

Photocatalysis is the generally accepted term for a process in which light and a catalyst bring about or accelerate a chemical reaction. The IUPAC definition states photocatalysis as 'a catalytic reaction involving light absorption by a catalyst or by a substrate' [1]. Photocatalysis can often be more accurately replaced by the term photosensitisation. This is a process by which a photochemical alteration occurs in one chemical species as a result of the initial absorption of radiation by another chemical species called the photosensitiser [2]. In semiconducting photocatalysis, no energy is stored, instead there is an acceleration of a reaction by a photon-assisted process. Titanium dioxide has been the practical photocatalyst [3] of choice for a variety of reactions due to its high stability and oxidising power. It functions by absorbing sub band-gap radiation, this generates an electron and positive hole that can migrate to the surface of the titania and promote oxidation and reduction reactions.

Powders and thin films of titania will photodegrade a wide range of organic and inorganic chemicals in air and water [4–6]. Other applications have included the elimination of microorganisms such as bacteria, [7–9] viruses, [10] cancer cells [11] and the reduction of trace heavy metals.

The main methods of generating $TiO_2$ nanocrystalline thin films [12] are chemical vapour deposition (CVD) [13,14] physical vapour deposition (PVD) [15], spin-coating and dip-coating [16–19]. $TiO_2$ photocatalytically active thin-films have been prepared from alkoxide solutions [17,19–23]. The latter, along with the source of titania, also determines the grain size, structure, phase and density of sol–gel derived films [24–27].

Although titania thin-films have been proven to be effective in photo-oxidising organic substances, they can only do so under sub approximately 350 nm radiation. Its band-gap of 3.2 eV means that anatase titania can use less than approximately 1% of the solar spectrum. Gerischer and Heller [28] have proposed that the activity of a photocatalyst is limited by the rate of electron

* Corresponding author. Tel.: +44-207-6794669; fax: +44-207-6797463
*E-mail address:* i.p.parkin@ucl.ac.uk (I.P. Parkin).

0277-5387/02/$ - see front matter © 2002 Elsevier Science Ltd. All rights reserved.
PII: S0277-5387(02)01333-5

transfer to oxygen on the surface of the catalyst. There has been some research [29–31] that suggests the modification of the $TiO_2$ surface by Noble metals such as Pd, Ag and Au, increases the efficiency of electron transfer to oxygen, which in turn increases the photo-oxidation efficiency. Some metals have also been doped into titania in order to improve its physical and optical properties [32].

There have recently been a number of reports on metal oxide doped-$TiO_2$ catalysts with the intention of improving photocatalytic activity and, in some cases, extending absorption into the visible light range. Some of the metal oxides that have been doped into $TiO_2$ are $SnO_2$, [33] $WO_3$ [27,34,33] $SiO_2$, $ZrO_2$ and $V_2O_5$. Tokumitsu et al. [36] have used $WO_3/TiO_2$ powdered photocatalysts to remove $(CH_3)_3N$, $CH_3SH$ and $CH_3CHO$ from air. Do et al. [21] have shown that the photo-oxidation of 1,4-dichlorobenzene was improved by adding $WO_3$ to the surface of $TiO_2$ powders.

The bandgap energy of $WO_3$ is 2.8 eV which falls within the solar spectrum. This combined with its physiochemical properties make it attractive for photo-catalysis research [34]. There have been different methods in preparing powdered $WO_3/TiO_2$ coupled semiconductor photocatalysts. The mixed oxide powder prepared by Do was made using an incipient wetness, ultrasonic nebulization and flame hydrolysis technique. Engweiler [34] used a multi-step grafting procedure using tungsten (VI)-oxo-methanolate and tungsten (V)-ethanolate as precursors to deposit tungsten oxide on top of a titania support. Recently, Li et al. [35] prepared $WO_3$–$TiO_2$ powder samples via a sol–gel process. They found that a 3% (M) doping of $WO_3$ into $TiO_2$ achieved the greatest activity in the destruction of methylene blue; its rate of photo-oxidation being greater than that of pure $TiO_2$. It was also confirmed that the mixed-oxide could be excited using visible light i.e. with $E < 3.2$ eV.

In addition to its photocatalytic activity $TiO_2$ thin films also demonstrate very hydrophillic surfaces after irradiation with ultra-band gap light. Thus, water droplets on $TiO_2$ coated glass usually exhibit a contact angle of 25°–35° before ultra band gap irradiation and less than 10° after. This phenomena, together with the photocatalytic effect of titania has enabled these films to be commercialised as self cleaning windows, for example Pilkington Active Glass [37,38].

In this paper we report the formation of thin films of titania, tungsten(VI) oxide and titania/tungsten(VI) composites from a sol–gel process. It was found that mixed films had marked self-cleaning properties including low-light induced superhydrophillicity and good photocatalytic response. Notably the doped tungsten oxide films were more efficient photocatalysts than equivalent titania films.

## 2. Experimental

### 2.1. Reagents

The following chemicals were used: Propan-2-ol, hydrochloric acid; tungsten (V) ethoxide $[W(OC_2H_5)_5]$ from Alfa Aesar; titanium tetraisopropoxide $[Ti(OCH(CH_3)_2)_4]$ and stearic acid from Aldrich.

### 2.2. Glass slide preparation

Standard microscope slides (BDH) $\sim 1$ mm thick and of dimensions $7.6 \times 2.6$ cm were used as the substrate. They were carefully cleaned prior to use by washing with distilled water, drying and finally washing with isopropanol before being left to air dry.

### 2.3. Preparation of the sols

#### 2.3.1. Transparent $TiO_2$ films

Titanium (IV) tetraisopropoxide (6.00 ml, 0.02 mol) was added to propan-2-ol (50 ml). HCl 2M (0.2 ml) was added drop-wise and the mixture was vigorously stirred for 1 h. The colourless clear solution was covered with a watch-glass and left overnight before use.

#### 2.3.2. $WO_3$ films

Tungsten pentaethoxide (0.900 g, 2 mmol) was added to propan-2-ol (50 ml). HCl 2M (0.15 ml, 0.03 mol) was added dropwise into the mixture under stirring. The pale yellow sol was stirred for 1 h and left for 24 h before use.

#### 2.3.3. $WO_3/TiO_2$ (2%) mixed oxide

Tungsten (V) ethoxide (0.164 g, 0.40 mmol) was added to titanium tetraisopropoxide (6.00 ml, 0.02 mol). Isopropanol (50 ml) was added to the mixture along with a few drops of 2M HCl. The slightly yellowish solution was stirred for 1 h and left overnight before use.

#### 2.3.4. $WO_3/TiO_2$ (6%) mixed oxide

Tungsten (V) ethoxide (0.489 g, 1.2 mmol) was added to titanium isopropoxide (6 ml, 0.02 mol). Isopropanol (50 ml) was mixed into the solution. HCl 2M (0.05 ml, 0.1 mmol) was added dropwise under stirring. The pale yellow solution was stirred for 1 h and left overnight before use.

#### 2.3.5. $WO_3/TiO_2$ (20%) mixed oxide

Tungsten (V) ethoxide (1.637 g, 4.0 mmol) was added to titanium isopropoxide (6 ml, 0.02 mol) to give a cloudy mixture. Isopropanol (50 ml) was stirred into the mixture along with a few drops of 2M HCl. The light yellow solution was stirred for 1 h and left overnight before use.

### 2.4. Dip-coating

The glass substrates were dipped in the solution by a locally constructed clipping machine. The withdrawal rate used for the single coated films was 60 cm $min^{-1}$. After each coat, the film was allowed to dry at room temperature for 10 min. The procedure was repeated to obtain multiple coatings. Different withdrawal speeds (0.5, 1, 3, 6, 12 and 60 cm $min^{-1}$) were used to produce a batch of single coated substrates whose photocatalytic activity, were then tested. The optimum time for ageing the solution was determined by obtaining dip coated samples every 1–2 days. Dip coated samples were obtained for up to 85 days after the intial mixing of reagents. The optimum coating was determined by assessing the photocatalytic response and contact angle.

### 2.5. Calcination

Samples were annealed in a furnace at 500 °C for 1 h in air to fully decompose the precursor and obtain crystalline samples. The rate of heating and cooling was 5 °C $min^{-1}$. The films that contained tungsten oxide were annealed under a stream of oxygen at 500 °C for 1 h.

### 2.6. Film characterisation

All of the samples were analysed whilst attached to the glass substrate.

X-ray powder diffraction patterns were measured on a Siemens D5000 diffractometer using monochromated Cu K$\alpha$1 radiation ($\lambda = 1.5406$ Å) in the reflection mode using glancing angle incidence (1.5°). Samples were indexed using Unit Cell and compared with database standards. SEM/EDAX was obtained on a Hitachi S570 instrument using the KEVEX system. Area mapping experiments were obtained on a Phillips ESEM instrument with an Oxford INCA EDX system and referenced against oxygen, titanium and tungsten standards. UV–Vis spectra were recorded in the range 200–1000 nm using a Helios single beam instrument. Reflectance and transmission spectra were recorded between 300 and 1100 nm by a Zeiss miniature spectrometer. The optical bandgaps for the titanium dioxide and tungsten oxide films were obtained from optical transmission measurements by plotting $(ahv)^{1/2}$ versus $hv$, where $a$ is the absorbance of the film ($a = -\log T/T_0$; $T$, sample optical transmission; $T_0$, substrate optical transmission) and $hv$ the photon energy [39]. Measurements were standardised relative to a rhodium mirror (reflectance) and air (transmission). Raman spectra were acquired on a Renishaw Raman System 1000 using a helium–neon laser of wavelength 632.8 nm. The Raman system was calibrated against the emission lines of neon. Contact angle measurements of selected glass samples was determined by measuring the size of a 7.5 μl droplet of water and applying a suitable program. Electrical conductivity was determined by a 4-probe device. Hardness scratch tests were conducted with felt pads, brass stylus and a stainless steel scalpel.

### 2.7. Photocatalytic activity measurements

The photocatalytic activity of the films was measured by the photodegradation of stearic acid. This organic compound was chosen because of its ease of oxidation and low vapour pressure. The overall reaction corresponds to:

$$C_{17}H_{35}COOH + 26O_2 \xrightarrow{TiO_2/hv} 18CO_2 + 18H_2O$$

Stearic acid (7.5 μml, 0.40 M solution in methanol) was placed on the surface of the film (2.6 × 2.6 cm) and spin coated at 1000 rpm for 20 s to obtain a dry, even coating. The integrated IR absorbance of the C–H stretching vibrations of stearic acid between 2850 and 2950 $cm^{-1}$ was measured using FTIR. The samples were then irradiated with a 254 nm ultra-violet lamp (BDH, 2 × 8 W germicidial lamp) at 20-min intervals for up to 1 h, or a 365 nm lamp (BDH 2 × 8 W black light bulbs) for 14 h. The integrated intensity of the C–H vibrations from the stearic acid overlayer was determined after every irradiation.

## 3. Results and discussion

### 3.1. Synthesis—$TiO_2$ films

Titanium isopropoxide was added to an acidic solution of isopropanol which was stirred for an hour and left to age overnight. The films were formed on the glass substrate by dipping into the aged sol and then withdrawing at a constant rate to obtain a uniform coating. The solution remained clear with no white $TiO_2$ microparticles precipitating out. Hydrochloric acid acts as a catalyst to complete the hydrolysis.

The probable mechanism for the process is shown in Scheme 1. The titanium alkoxide is protonated in a rapid first step. This makes the Ti atom more electrophilic and susceptible to attack form the water [16]. Withdraw of the glass-slide from the fluid–sol produces a transparent film due to the evaporation of the solvent and hydrolysis of [Ti-($O^iPr$)$_4$]. During dipping, aggregation, gelation and drying occurs in seconds to minutes, rather than days as in bulk sol–gel systems [23]. Annealing of the film removed any remaining solvent and the structure is stiffened i.e. a Ti–O–Ti network formed by removal of the alkoxy and hydroxyl groups to produce an anatase thin film. It was noted that the

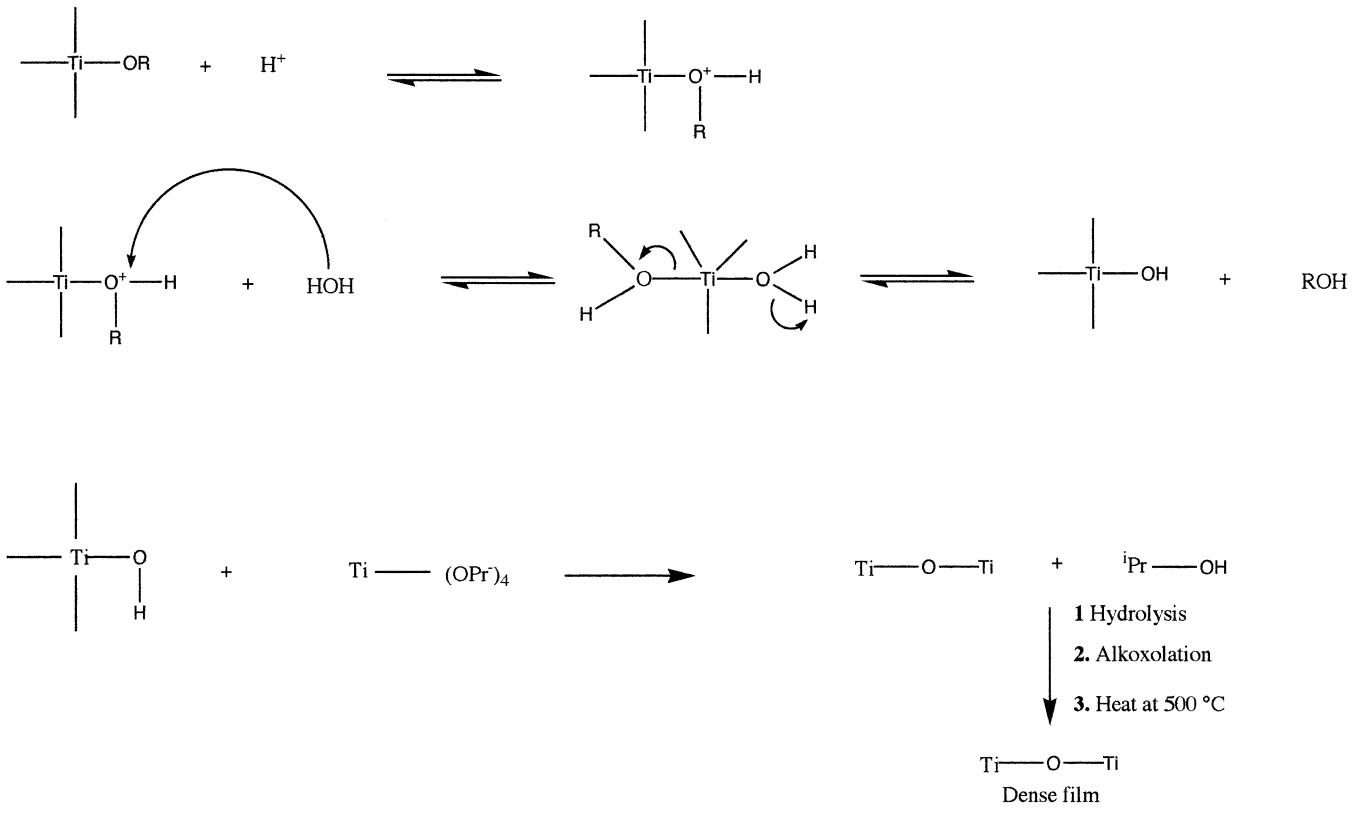


Scheme 1.

most photocatalyically active films were formed by dip-coating 24 h after the initial hydrolysis.

### 3.2. Synthesis—$WO_3/TiO_2$ mixed oxide and $WO_3$ films

Tungsten (V) ethoxide and titanium isopropoxide were mixed into an acidic solution of isopropanol which was stirred for an hour and left overnight to age. The films were prepared exactly as for the $TiO_2$ ones. The addition of tungsten oxide to the titania can result in two sorts of films where the tungsten has been incorporated into the $TiO_2$ to form a solid solution $Ti_xW_yO_2$ or the two components exist in separate phases $WO_3$ and $TiO_2$. The tungsten oxide films were prepared in the same manner as the mixed oxide films.

### 3.3. Physical properties of the films

The single coated mixed oxide and $TiO_2$ films after annealing at 500 °C were quite robust and resistant to peeling with Scotch Tape and scratching with a fingernail and brass stylus. All films could be scratched with a stainless steel scalpel. The $WO_3$ films were less robust. An increased number of coatings on the substrate led to the film becoming less resistant to scratching for all films. This is due in part to the increased number of cracks that appear on the surface as thicker films are obtained from multiple dip-coating. Annealing the films produced in this study did cause further shrinkage and cracking at the surface.

### 3.4. Visual appearance

The single coated films from all of the doped and undoped systems were optically transparent and uniform. Increasing the number of dip coatings produced opaque films. This was due to an increase in coating thickness and the affects of atmospheric humidity, which hydrolysed the alcoholate-adsorbed layer.

The speed with which the substrate is withdrawn from the solution affects the thickness of the film produced. From the electronic spectra it was found that the fastest withdrawal rate produced the thickest film. This observation has also been reported by other researchers [22] who suggest that a high dipping speed produces comparatively thick coatings. The slower the withdrawal speed, the greater the overlap of the deposition and drying stages [23]. Therefore, there is competition between evaporation, which compacts the film and continued condensation reactions, which stiffens the film and increases its resistance to compaction. It was found that optimum film properties were obtained with a withdraw speed of 3 cm $s^{-1}$. At this withdraw speed, SEM indicated that the thickness of the film increased by approximately 250 nm per dip coat.

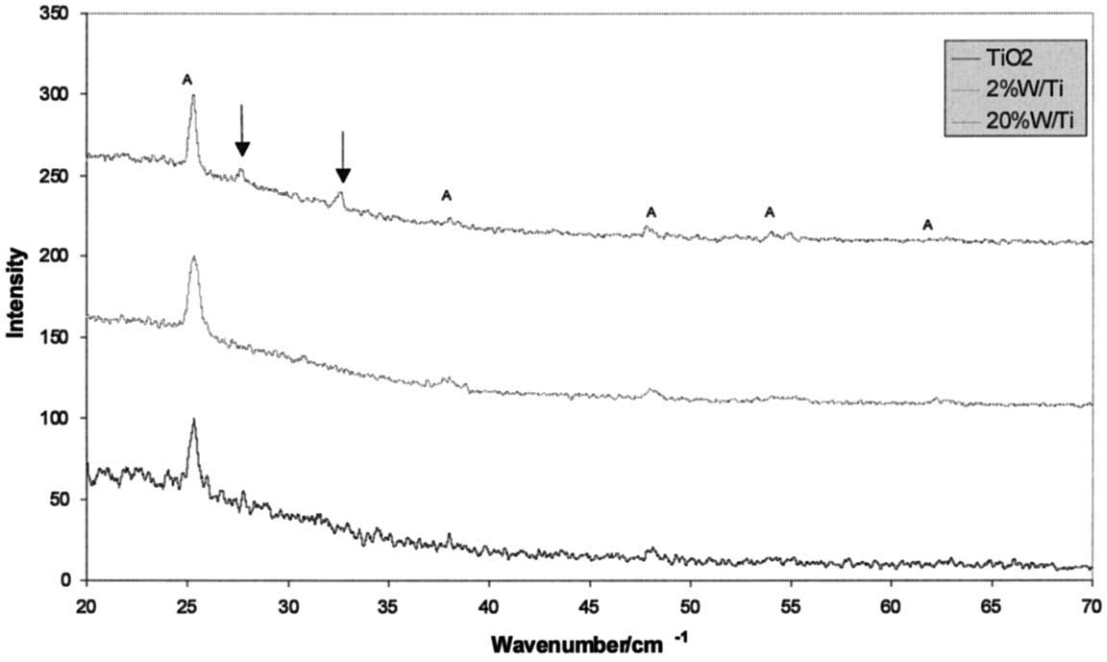


Fig. 1. X-ray powder diffraction patterns from the annealed films formed by dip-coating; bottom trace-$TiO_2$ film; middle trace 2% $WO_3$–$TiO_2$; top trace 20% $WO_3$–$TiO_2$. Peaks marked with A correspond to the anatase form of titania, peaks marked with an arrow represent monoclinic $WO_3$.

### 3.5. X-ray powder diffraction

Analysis of all of the annealed $TiO_2$ and tungsten oxide doped $TiO_2$ films by X-ray powder diffraction gave the pattern for the anatase form of $TiO_2$. The most intense reflection at 25.3° is assigned to the (1 0 1) plane of anatase, Fig. 1 [40]. There are no peaks that correspond to the presence of rutile [41]. Notably the anatase peaks remain invariant with position on increasing tungsten doping. This implies that tungsten is not entering the anatase phase to any measurable extent to form a solid solution. There are no extra reflections observed due to an identifiable $WO_3$ phase for the 2 and 6% doped samples. In the highest tungsten loaded titania film (20% $WO_3/TiO_2$), there are two additional peaks at $2\theta = 27.8°$ and 32.6°, represented by the arrows in Fig. 1. These can be assigned to orthorhombic $WO_3$. Orthorhombic $WO_3$ is formed conventionally by heating amorphous $WO_3$ at a temperature between 320–720 °C [41].

### 3.6. Raman analysis

The Raman spectrum for the $TiO_2$ films showed peaks at 144, 202, 401, 522 and 643 $cm^{-1}$ which are directly attributable to anatase (literature values: [42]

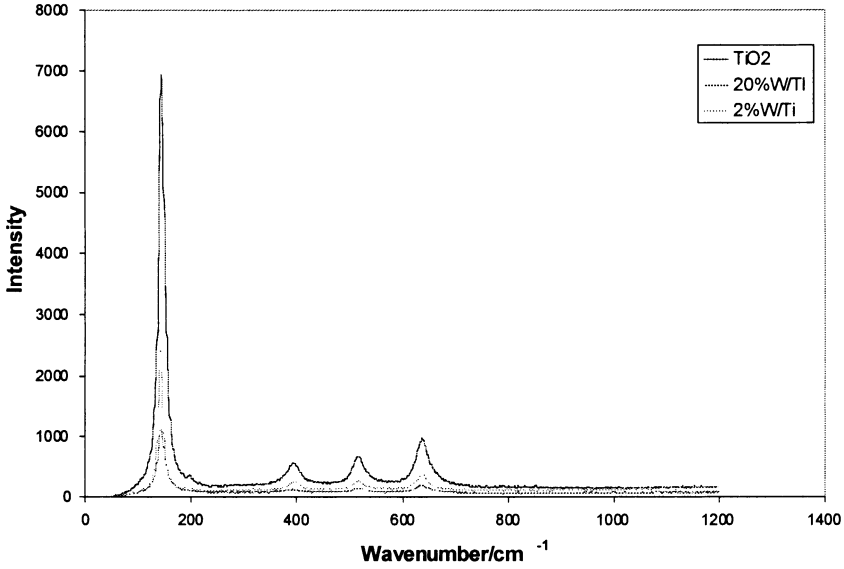


Fig. 2. Raman patterns for annealed sol–gel derived films of $TiO_2$; 2% $WO_3$–$TiO_2$ and 20% $WO_3$–$TiO_2$.

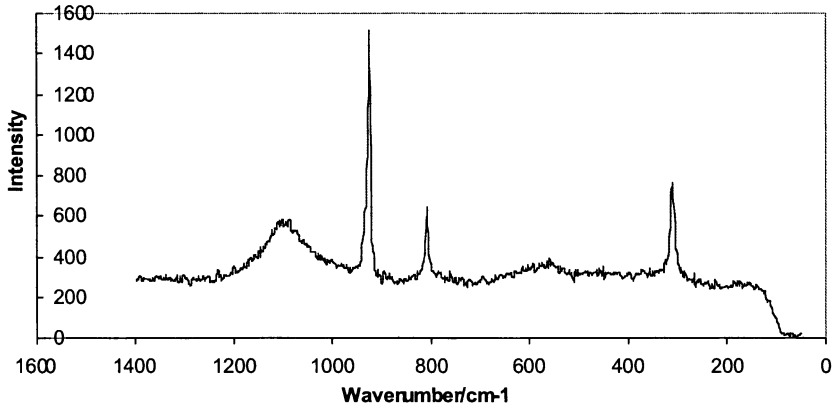


Fig. 3. Raman pattern for annealed sol–gel derived $WO_3$ film.

143, 396, 516, 639 $cm^{-1}$). There are no peaks that indicate the presence of rutile $TiO_2$ [42]. The Raman spectra for the 2, 6 and 20% $WO_3/TiO_2$ films are shown in Fig. 2 and are identical to anatase. There were no additional peaks detected. There were also no shifts in the Raman peaks which would point to the incorporation of $WO_3$ into the titania as in the formation of a solid solution. Notably titania is very efficient at Raman scattering and the presence of the much weaker Raman scatterer $WO_3$ would be lost into the relative background count at 2–20% doping. However the Raman spectrum for the pure tungsten oxide film showed sharp peaks at 309, 808 and 924 $cm^{-1}$, Fig. 3. These are attributed to crystalline orthorhombic $WO_3$, which shows sharp bands at 807 $cm^{-1}$ and in the range 240–350 $cm^{-1}$. The bands at 309 and 808 $cm^{-1}$ are due to the O–W–O bending and stretching modes, respectively. The band at 924 $cm^{-1}$ is due to the terminal W=O bond, which is common for all types of tungsten trioxides [34].

### 3.7. EDX and SEM analysis

The EDX elemental analysis of the various films gives Ti:W ratios that are directly comparable with the amount of precursors initially used (within 0.3 atom%). Notably only oxygen, titanium and tungsten were observed by EDX. Therefore, there was very good elemental composition transferability from the solution to the deposited films. Multiple spot analysis with a 1 μm spot size on all of the doped films showed a homogeneous dispersion of tungsten throughout the film. An elemental surface map of the 20% $WO_3/TiO_2$ film was obtained. This map also showed that there is a homogeneous distribution of titanium, tungsten and oxygen within the film. On the scale of the EDX measurements (ca. 1 μm resolution) the Ti and W are fully intermixed. No individual particles could be identified as being either pure $TiO_2$ or $WO_3$; this indicates that the tungsten oxide is well distributed with the titania particles. These results combined with the XRD and Raman results indicate that the tungsten is not entering the anatase phase to any measurable extent to form a solid solution.

### 3.8. Electronic spectra

The electronic spectrum for an annealed single dip-coated $TiO_2$ film shows an absorption band edge at 350 nm. This is due to the $O^{2-} \rightarrow Ti^{4+}$ charge transfer in anatase [38]. The apparent shift of absorption as the films increase in thickness is due to light scattering effects. There are also some very weak bands around 400–600 nm due to interference fringes.

The electronic spectrum of the $WO_3$ doped material shows a large band that is due to $TiO_2$ and has an absorption edge of 350 nm. There is also a smaller band that has a maximum of 390 nm and an absorption edge of 460 nm, this is due to the $O^{2-} \rightarrow W^{6+}$ transition [34]. The absence of significant absorptions in the visible region due to $d$–$d$ transitions points to the absence of reduced W species with respect to the $d^0$ hexavalent state of $W^{6+}$ [34]. The band gap energy of $TiO_2$ was determined by optical transmission measurements at 3.2 eV and exactly matches that of anatase $TiO_2$. Equivalent measurements on the pure $WO_3$ dip-coated films gave a bandgap of 2.8 eV, which corresponds to monoclinic tungsten trioxide [3].

### 3.9. Photocatalysis measurements

The photocatalytic activities of all of the films was determined by the photodegradation of a thin spin-coated film of stearic acid. The IR absorbance of the C–H stretches of stearic acid was measured using FTIR. The change in area of the peaks was calculated after each irradiation with 254 nm light. The decrease in the C–H peak area of stearic acid as a function of irradiation time is given in Fig. 4 for a series of $TiO_2$ films with increasing thickness. The most photocataly-

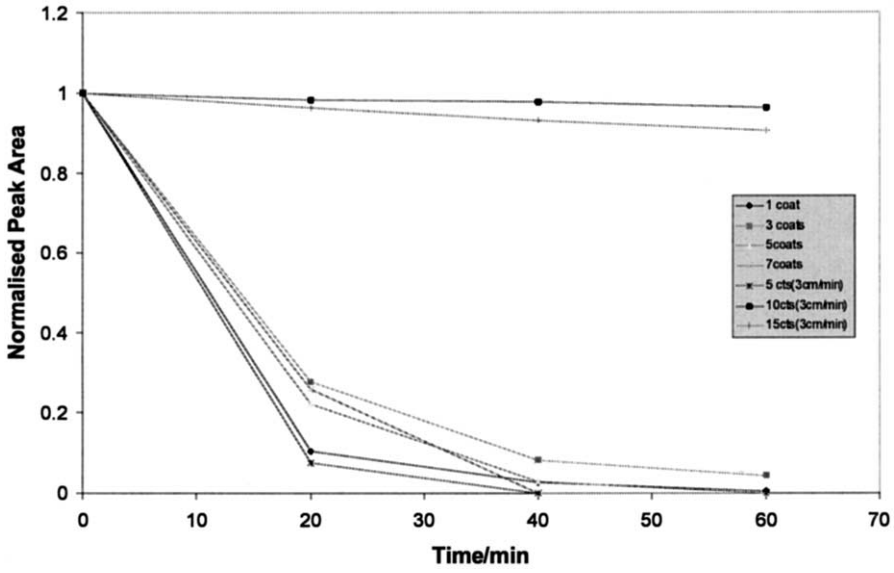


Fig. 4. Change in integrated intensity of the C–H streching region of stearic acid (2950–2800 $cm^{-1}$) against irradiation time (min, 254 nm) for annealed $TiO_2$ dip coated films of different thicknesses (1 dip coat ca. 250 nm).

tically active titania film consisted of three dip-coats. This is probably due to the greater amount of titanium dioxide available to participate in the photocatalytic reaction. For this sample, 80% of stearic acid was removed after 40 min of illumination at 254 nm. A blank of uncoated glass showed no loss of stearic acid over the same period. However, under these irradiation conditions, increasing the number of coats after three did not result in an increase in the photodegradation rate. This could be due in part to the increase in opacity and light scattering of thick $TiO_2$ films.

Fig. 5 shows the photocatalytic activity of 2% $WO_3$/$TiO_2$ films of different thicknesses. The most active film was the five dip coated one prepared using a withdrawal speed of 3 cm $min^{-1}$ (ca. 1 μm thick). The ten and 15-coated samples (corresponding to ca. 2.0 and 3.0 μm) using the same withdrawal speed were not nearly as active as the others showing that increased thickness of the film above a certain optimum point does not necessarily accompany increased photoactivity. In the five-coated sample, the amount of stearic acid decreased to nearly zero after 40 min of UV illumination.

A comparative study was also undertaken to determine the activity of 2, 6 and 20% $WO_3/TiO_2$ films for the destruction of stearic acid using 365 nm irradiation. These results showed that all of the doped films were active in the destruction of a stearic acid overlayer. The most active photocatalyst was the 2% doped tungsten system, Figs. 5 and 6. A comparision was also made between films obtained from a single dip coating and

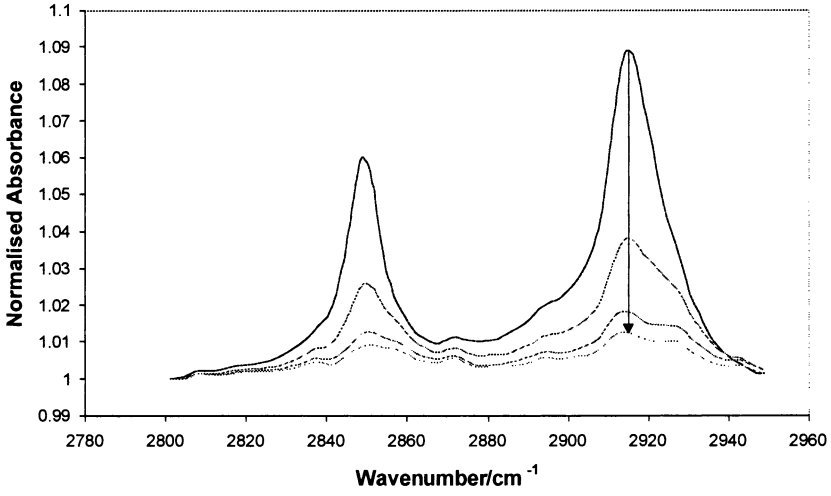


Fig. 5. Change in integrated intensity of the C–H streching region of stearic acid (2950–2800 $cm^{-1}$) against irradiation time (min, 254 nm) for annealed 2% $WO_3$ doped $TiO_2$ dip-coated films of different thicknesses and withdraw speeds.

those formed from three dip coats. In all cases the thicker three dip coated film was the most active photocatalyst. The fact that these coatings show activity with 365 nm radiation indicates that they have potential as active photocatalysts using sunlight. Notably the rate of photodestruction using 365 nm radiation was significantly less than that for 254 nm radiation. Experiments using filters would be required to ensure that the activity was actually due to the longer wavelengths emitted by the 365 nm lamp as unlike the 254 nm lamp

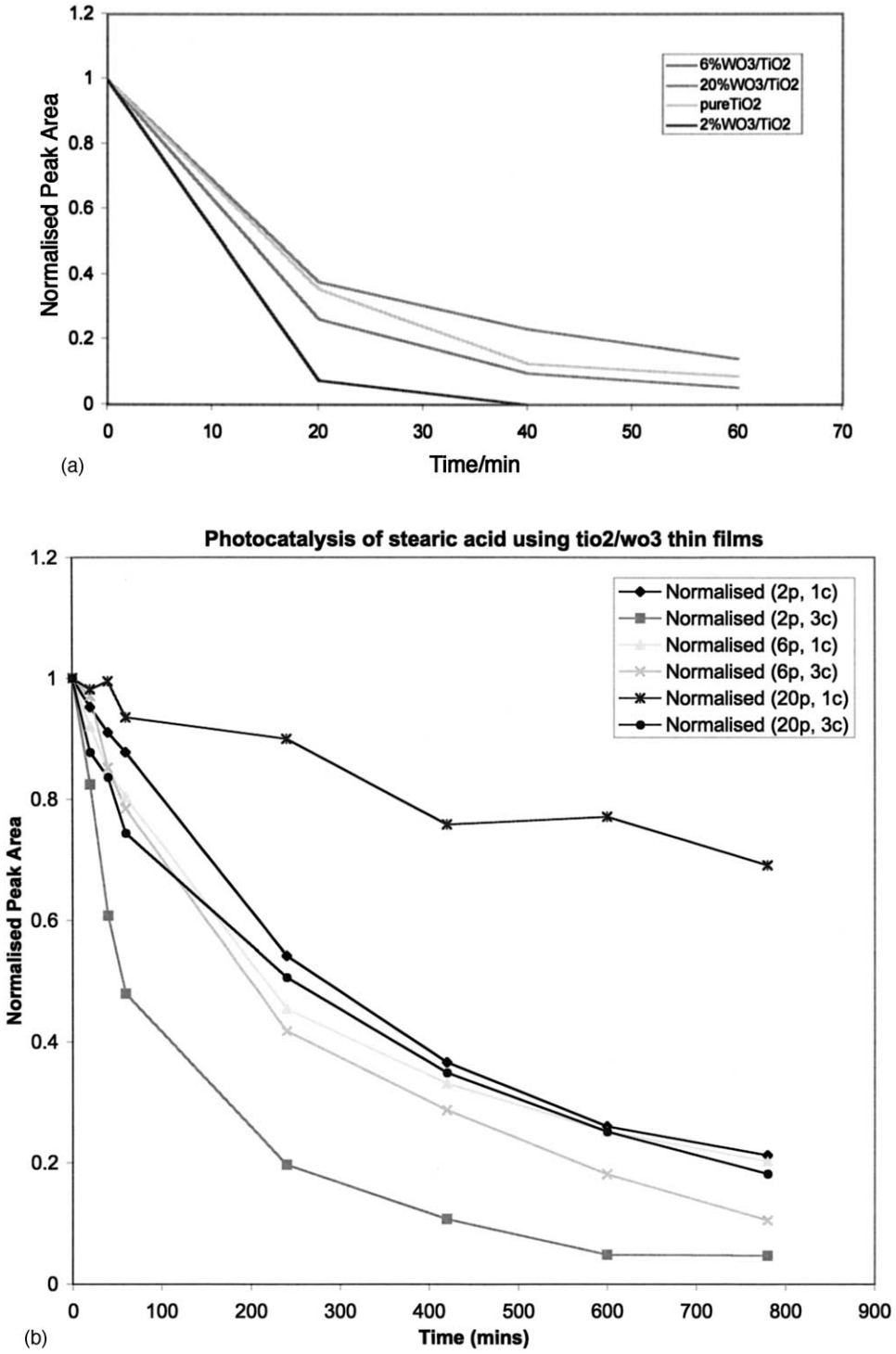


Fig. 6. (a) Change in integrated intensity of the C–H streching region of stearic acid (2950–2800 $cm^{-1}$) against irradiation time (min, 254 nm) for annealed $WO_3$ doped $TiO_2$ dip coated films of equivalent thickness (1 μm). (b) Change in integrated intensity of the C–H streching region of stearic acid (2950–2800 $cm^{-1}$) against irradiation time (min, 365 nm) for annealed $WO_3$ doped $TiO_2$ dip coated films of equivalent thickness (1 μm). 2p = 2% $WO_3$ in $TiO_2$; 1c = one dip coat.

the emmision spectrum has a tail in both the visible and UV portions of the spectrum.

The photoactivity of the dip coated films is quite remarkable. Direct literature comparisons are difficult to obtain because of the use of a multitude of different standards. However, in a recent paper, [34] it was reported that $WO_3$ doping did not enhance the photocatalytic oxidation activities of $TiO_2$ at all. Another paper [43] reported a 65% decrease of $8.8 \times 10^{-3}$ M stearic acid after 30 min of irradiating a $TiO_2$ thin film with 254 nm radiation.

### 3.10. Accounting for the changes in photoactivity

The absence of tungsten oxide peaks in the XRD spectra for the most active film (2% $WO_3/TiO_2$) suggests that the increased photoactivity, with respect to $TiO_2$, is not due to the formation of crystalline tungsten oxide but is probably due to $WO_3$ acting as a separation centre for the electrons and holes. The bandgap energy of $TiO_2$ anatase is 3.2 eV and that of monoclinic $WO_3$ is 2.8 eV. The flat band potentials of $TiO_2$ and $WO_3$ are $-0.1$ and $+0.5$ V (vs. normal hydrogen electrode at pH 0), [34] (Scheme 2).

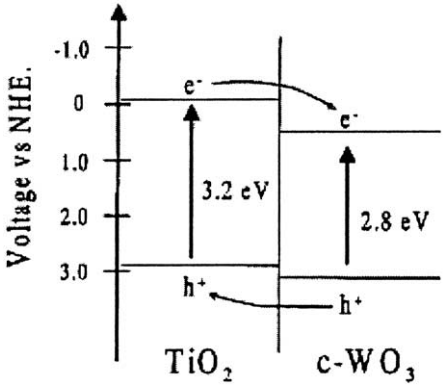


Scheme 2. Energy diagrams for $WO_3/TiO_2$ films.

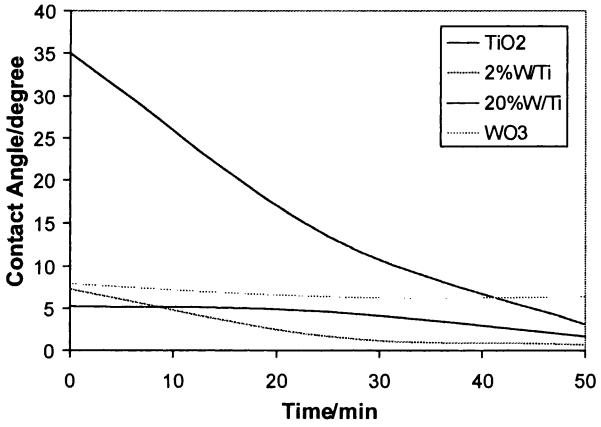


Fig. 7. Contact angle (°) against irradiation time (min, 254 nm) for $TiO_2$, 2 and 20% $WO_3$–$TiO_2$ and $WO_3$ films.

The conduction and valence bands of $WO_3$ are lower in energy than those of $TiO_2$. When optical excitation occurs, the photogenerated electrons will be transferred to the lower-lying conduction band of $WO_3$, while the holes will accumulate in the valence band of $TiO_2$. Thus $WO_3$ acts as an effective separation centre and the photogenerated electrons can be transferred to the surface, rather than undergoing bulk recombination, where they will react with adsorbed species such as oxygen and hence increase the rate of photo-oxidation.

### 3.11. Contact angle changes

Contact angle measurements were carried out to determine the wettability change of the $TiO_2$ surface under UV illumination. There are few materials that exhibit water contact angles of less than 10° except porous ones. Fig. 7 shows the change in contact angle as the various samples are irradiated with 254 nm light. The films were irradiation at 20 min burst intervals for upto 1 h. This was sufficient to give rise to a hydrophilic surface where the contact angle with water was less than 5°. This phenomenon did not last indefinitely and the surface gradually returned to its hydrophobic state after storage in the dark over 24 h. The 2% $WO_3/TiO_2$ film exhibited a more hydrophilic surface than the pure $TiO_2$ and 20% $WO_3/TiO_2$ film. Other researchers [34] have also found that the addition of tungsten oxide to titanium dioxide powders enhances its hydrophilic effect, however, as the amount of deposited $WO_3$ exceeded 1.0 wt.%, it began to decrease. The pure $WO_3$ and the highest tungsten loading (20% $WO_3$) films showed the least change in contact angle. This probably means that even though $WO_3$ enhances the effect on the $TiO_2$ surface, the $WO_3$ itself does not become hydrophilic.

The photocatalytic effect and the photoinduced hydrophilic effect both occur at the same $TiO_2$ surface and have a common source [34]. Photocatalysis involves the reaction of the photogenerated electrons with $O_2$ to produce the superoxide radical anions which when combined with hydroxyl radicals attack organic compounds. Contact angle changes are due to generation of hydroxylated $TiO_2$ surfaces.

## 4. Conclusion

Titanium dioxide thin films were made in the most photoactive form-anatase by dip-coating from an acidified alkoxide precursor. The photoactivity activity of the films in destroying an overlayer of stearic acid increased with film thickness. An optimum thickness of around three dip-coated layers was required for maximum photoactivity. Composites of 2%, 6% and 20% tungsten trioxide in titania were made in which the

tungsten trioxide was found to be highly dispersed in the titania phase. However, a solid solution did not form as seen from the EDAX surface mapping results, Raman spectra and XRD patterns. Increasing the tungsten loading shifted the electronic absorption edge towards the visible region. The $TiO_2$, 2% and 6% films demonstrated a photoactivated superhydrophillic effect, as the contact angle of water on their surfaces was greatly reduced after irradiation with UV light. Notably 2% $WO_3$ doped titania showed the lowest contact angles. Composite $WO_3/TiO_2$ films were found to increase the photocatalytic activity of $TiO_2$. The optimum doping for these sol–gel produced films was found to be 2% M $WO_3$. The enhanced photoactivity of the doped films was accounted for in terms of a charge separation model. These doped films show great potential for self-cleaning applications such as windows as they show lower contact angles than pure titania and are more effective in removing a test organic–stearic acid.

## Acknowledgements

The EPSRC is thanked for financial support. Pilkington Glass are thanked for useful discussions on related projects.

## References

[1] A. Mills, S. Le Hunte, J. Photochem. Photobiol. A: Chem. 108 (1997) 1.
[2] A. Fujishima, K. Honda, Acc. Chem. Res. 28 (1995) 3.
[3] M. Kamei, T. Mitsuhushi, Surf. Sci. L609 (2000) 463.
[4] S. Hager, R. Bauer, G. Kudielka, Chemosphere 41 (2000) 1219.
[5] A. Topalov, D. Molnar-Gabor, M. Kosanic, B. Abramovic, Water Res. 34 (2000) 1473.
[6] T.N. Obee, S. Satyapal, J. Photochem. Photobiol. A: Chem. 118 (1988) 45.
[7] Z. Huang, P.C. Maness, D.M. Blake, E.J. Wolfrum, S.L. Smolinski, W.A. Jacoby, J. Photochem. Photobiol. A: Chem. 130 (2000) 163.
[8] W.A. Jacoby, P.C. Maness, D.M. Blake, E.J. Wolfrum, J.A. Fennell, Environ. Sci. Techol. 32 (1998) 2650.
[9] J.C. Ireland, P. Klostermann, E.W. Rice, R.M. Clark, Appl. Environ. Microbiol. 59 (1993) 1168.
[10] J.C. Sjogren, R.A. Sierka, Appl. Environ. Microbiol. 60 (1994) 344.
[11] R. Cai, K. Hashimoto, K. Itoh, Y. Kubota, A. Fujishima, Bull. Chem. Soc. Jpn. 64 (1991) 1268.
[12] I. Sopyan, M. Watanabe, S. Murasawa, K. Hashimoto, A. Fujishima, J. Photochem. Photobiol. A: Chem. 98 (1996) 79.
[13] C. Otterman, K. Bange, Thin Solid Films 15 (1996) 245.
[14] K. Segawa, M. Katsuta, F. Kameda, Catal. Today 29 (1996) 215.
[15] S. Amor, G. Baud, J. Besse, J. Jacquet, Mater. Sci. Eng. 47 (1997) 110.
[16] I. Sopyan, M. Watanabe, S. Murasawa, K. Hushimoto, A. Fujishima, Chem. Lett. (1996) 69.
[17] N. Negishi, T. Iyoda, K. Hashimoto, A. Fujishima, Chem. Lett. (1995) 841.
[18] Y. Paz, Z. Luo, L. Rabenberg, A. Heller, J. Mater. Res. 10 (1995) 2842.
[19] Y. Paz, A. Heller, J. Mater. Res. 12 (1997) 2759.
[20] I. Strawbridge, P.F. James, J. Non-Cryst. Solids (1986) 381.
[21] A. Fernadez, G. Lassaletta, V.M. Jimenez, A. Justo, A.R. Gonzalez-Elipe, J.-M. Hermann, H. Tahiri, Y. Ait-Ichou, Appl. Catal. B: Environ. 7 (1995) 49.
[22] J. Yu, X. Zhao, Mater. Res. Bull. 35 (2000) 1293.
[23] C.J. Brinker, G.W. Scherer, The Physics and Chemistry of Sol–Gel Processing, Academic Press, New York, 1990.
[24] V. Kozhukharov, C. Trapalis, B. Samuneva, J. Mater. Sci. 28 (1993) 1283.
[25] M. Rahman, G. Yu, T.S. Soga, T. Jimbo, H. Ebisu, M. Umeno, J. Appl. Phys. 88 (2000) 4634.
[26] J. Yuan, S. Tsujikawa, J. Electrochem. Soc. 142 (1995) 3444.
[27] Y.R. Do, W. Lee, K. Dwight, A. Wold, J. Solid State Chem. 108 (1994) 198.
[28] H. Gerischer, A. Heller, J. Phys. Chem. 95 (1991) 5261.
[29] J. Papp, H.-S. Shen, R. Kershaw, K. Dwight, A. Wold, Chem. Mater. 3 (1993) 284.
[30] I. Izumi, W.W. Dunn, K.O. Wilbourne, F.F. Fan, A.J. Bard, J. Phys. Chem. 84 (1980) 3207.
[31] W. Lee, H.-S. Shen, K. Dwight, A. Wold, J. Solid State Chem. 106 (1993) 288.
[32] M. Rahman, T. Miki, K. Krishna, T. Soga, K. Igarashi, S. Tanemura, M. Umeno, Mater. Sci. Eng. B41 (1996) 71.
[33] M. Takahashi, K. Mita, H. Toyoki, M. Kume, B. Idriss, P.V. Kamat, J. Phys. Chem. 599 (1995) 9182.
[34] (a) B. Idriss, P.V. Kamat, J. Phys. Chem. US 99 (1995) 9182;
(b) J. Engweiler, J. Harf, A. Baiker, J. Catal. 159 (1996) 259;
(c) A. Fujishima, D.A. Tryk, T. Watanabe, K. Hashimoto, Int. Glass Rev. (1998) 114;
(d) D.A. Tryk, A. Fujishima, K. Honda, Electrochim. Acta (2000) 2363;
(e) R. Wang, K. Hashimoto, A. Fujishima, M. Chikuni, E. Kojima, A. Kitamura, M. Shimohigoshi, T. Watanabe, Adv. Mater. 10 (1998) 135;
(f) G.R. Bamwenda, K. Sayama, H. Arakawa, J. Photochem. Photobiol. A: Chem. 122 (1999) 175;
(g) L.J. Alemany, L. Lietti, N. Ferlazzo, P. Forzatti, G. Busca, E. Giamello, F. Bregani, J. Catal. 155 (1995) 117.
[35] X.Z. Li, F.B. Li, C.L. Yang, W.K. Ge, J. Photochem. Photobiol. A: Chem. 141 (2001) 209.
[36] S. Tokumitsu, N. Naruo, M. Fukunaga, T. Ikeda, Jpn. Kokai Tokkyo Koho JP 01, 159, 030 1989.
[37] http://www.toto.co.jp; http://pilkington.com.
[38] A. Fujishima, N. Tata, D.A. Tryk, Electrochim. Acta 45 (2000) 4683.
[39] J. Fix, Chem. Mater. 3 (1991) 1140.
[40] J. Mater. Sci., 24 (1989) 243
[41] Y.H. Chee, R.P. Cooney, R.F. Howe, P.A.W. van der Heide, J. Raman Spectrosc. 23 (1992) 161.
[42] Z. Pinter, Z. Sassi, S. Kornely, C. Pion, I.V. Perczel, K. Kovacas, R. Bene, J.C. Bureau, F. Reti, Thin Solid Films 391 (2000) 243.
[43] R. Fretwell, P. Douglas, J. Photochem. Photobiol A: Chem 143 (2001) 229.